Finite element simulation of multistage wire drawing processes of unalloyed carbon steels

M. Sc. Christian Otto

Department of Mechanical Engineering, Institute for Design and Precision Engineering
Machine Elements Group, Technische Universität Ilmenau, Germany

ABSTRACT

The paper deals with the finite element simulation of wire drawing processes with focus on unalloyed carbon steels. Based on the development of suitable material models as a basis for the simulation model, the forming processes are analyzed over several drawing stages for different drawing regimes. The simulation model is validated by comparing the simulation results with measured values. For the description of the forming behavior, the damage developments of the wire during the multi-stage forming are specifically analyzed. Subsequently, forming limits are derived by correlating the calculated damage with mechanical parameters of the wires. The validation of the damage models used is made possible by an FE parameter study, within which a targeted variation of the drawing die geometry takes place at a specific drawing stage. The paper is concluded by the verification of the results obtained theoretically by practical tests on a wire drawing machine using critical drawing die geometries.

1. INTRODUCTION

The production of high-strength, patented drawn steel wire forms the basis for numerous technical applications, which are used worldwide. High-strength wires are used, among other things, to produce technical springs for automotive and mechanical engineering, tire insert wires and ropes for a wide range of applications. The starting material for steel wire production is usually wire rod, which is drawn to the required nominal diameter over several drawing stages. Due to the increasing hardening of the wire, heat treatment (lead bath patenting) is necessary after a certain drawing stage to allow further forming of the wire. In order to save the associated high costs, an optimization of the wire drawing process with regard to the maximum possible forming without lead bath patenting is aimed at [4]. The use of the finite element method is the most effective way to achieve this goal.

2. FE SIMULATION MODEL

The realized drawing process has a decisive influence on the mechanical properties of the wires as well as on the economy of production. The wire drawing process is influenced by a large number of parameters. However, a complete experimental investigation with regard to the existing parameters is very time-consuming and not possible in every case. For this purpose, an FE simulation model is being developed with ANSYS, which is intended to simulate the real drawing process. The FE simulation offers various advantages:

- Modeling of all physical interactions in the forming process and coupled calculation
- Quantitative mapping of the real forming processes => detailed spatially resolved analysis
- Short computation times => automated calculation of numerous simulation variants in reasonable time periods possible, which in practice would not be feasible in part without a considerable expenditure of time

– Comparison and evaluation of different drawing regimes through analysis of selected results

2.1 Structure of the simulation model

The simulation model consists of a wire section and several drawing dies arranged one after the other. The wire is drawn through the dies one after the other and deformed further and further until the desired final diameter is reached. To reduce computation times, an axially symmetric 2D model is chosen for the wire. The drawing dies are modeled as rigid line models. The coefficient of friction in the contact area between wire and die is set depending on the drawing stages. Figure 1 shows the schematic structure of the simulation model.

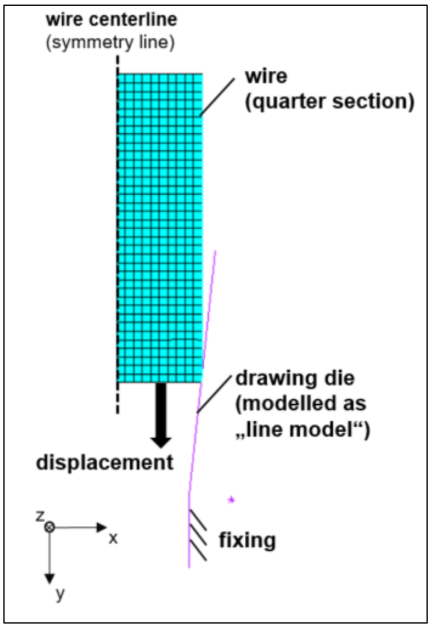

Figure 1: Schematic structure of the simulation model

Due to the process-related large degrees of deformation, large mesh distortions occur during the simulation. In order to ensure convergence of the numerical calculation, the simulation model is remeshed at regular intervals. A total of four different drawing sequences of wires are simulated, each with three different carbon contents (0.48% - 0.82%). The drawing sequence is defined by the respective individual cross-section reductions, the total cross-section reduction, the number of drawing stages and the drawing die geometries.

2.2 Material model

The basis of the simulation is a material model, which includes the definition of the stress-strain curve and the hardening model. To determine the stress-strain curve, wires are produced on real drawing machines and samples are taken from each drawing stage. Tensile tests (using tensile testing machines, according to [2]) are then carried out on the drawn wires. The 0,2% - yield strength $R_{p0,2}$ of the wire is obtained for each drawing stage. The values of $R_{p0,2}$ are then plotted versus the plastic strain, resulting in the stress-strain curve of the wire.
The determination of the $R_{p0,2}$ values from the tensile tests is not readily possible for the drawn wires. The reason for this is the process-related pre-curvature of the wires. When the wires are chucked, they are forced in the axial direction, inserting bending stresses into the wire. These bending stresses and the residual stresses from the wire drawing process are superimposed on the tensile load stress of the tensile test.

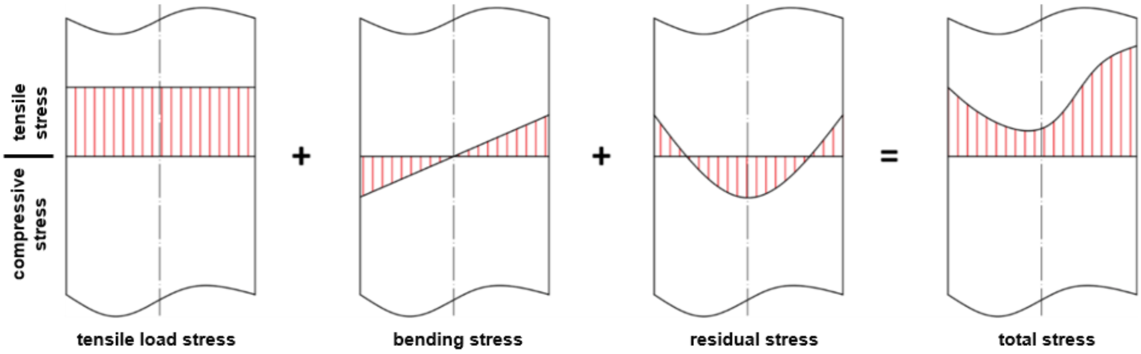

Figure 2: total stress from tensile load stress, bending stress and residual stresses (course assumed)

This leads to the fact that some areas of the wire start to deform plastically sooner. As a result, no linear elastic range can be derived from the characteristic curve, which is a prerequisite for determining the $R_{p0,2}$ values. To solve this problem, a calculation tool was developed in the Department of Machine Elements at the Ilmenau University of Technology, with which the bending stress influences can be eliminated [7]. For a correct determination of the stress-strain curves, the calculation tool was applied to the still relatively soft, strongly pre-curved thick wires of the first five drawing stages, since the influence of the residual bending stresses is greatest here. Regarding the higher drawing stages, the $R_{p0,2}$-values could be taken directly from the tensile tests. The result was a corrected stress-strain curve for each drawing sequence and carbon content. Based on these corrected stress-strain curves, averaged stress-strain curves for the wires of each carbon content were developed to improve the comparability of the simulation results and the convergence behavior of the simulation. In Figure 3, the three averaged stress-strain curves of the wires of the respective carbon contents are shown (for example, C82 means 0.82% carbon content).

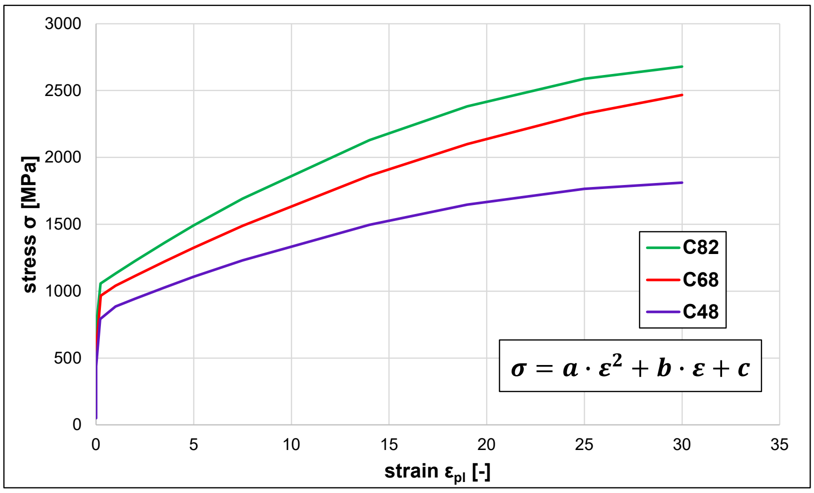

Figure 3: average stress-strain curves C48, C68 and C82

2.3 Validation of the simulation model

For validation of the simulation model, comparisons are made between the calculated and measured drawing forces and temperatures. Both variables are measured on the drawing machine in-line during wire drawing. The respective no-load components of the drawing forces can be determined from the machine data. The drawing machine used operates with a counter-drawing technique. The counter-draw components at each drawing stage are also determined from the machine data and taken into account in the FE simulation model. This ensures comparability between simulation and measurement with regard to the drawing forces.

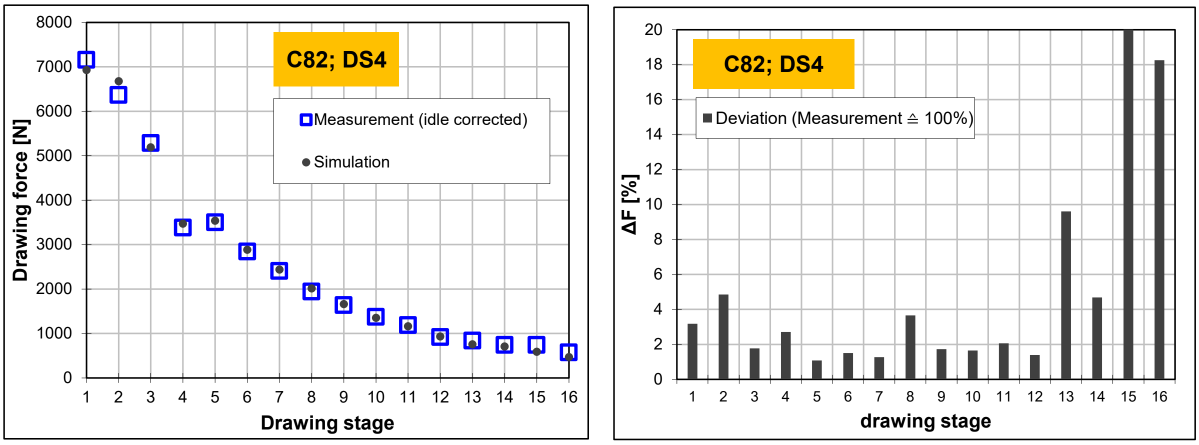

Figure 4: Drawing force comparison measurement and simulation

Up to drawing stage 14, the percentage deviations are on average approx. 2%, and approx. 4% when considered over all wires of the three carbon fractions. With the exception of the last two drawing stages, the drawing forces from simulation and measurement show very good agreement.

The wire temperatures during the wire drawing process are measured with an IR camera. The measurement is taken at the wire surface shortly after the wire exits the drawing die. Figure 5 shows the respective temperature curves and the percentage deviations (measurement = 100%) for two different numbers of drawing stages ("DS" for short).

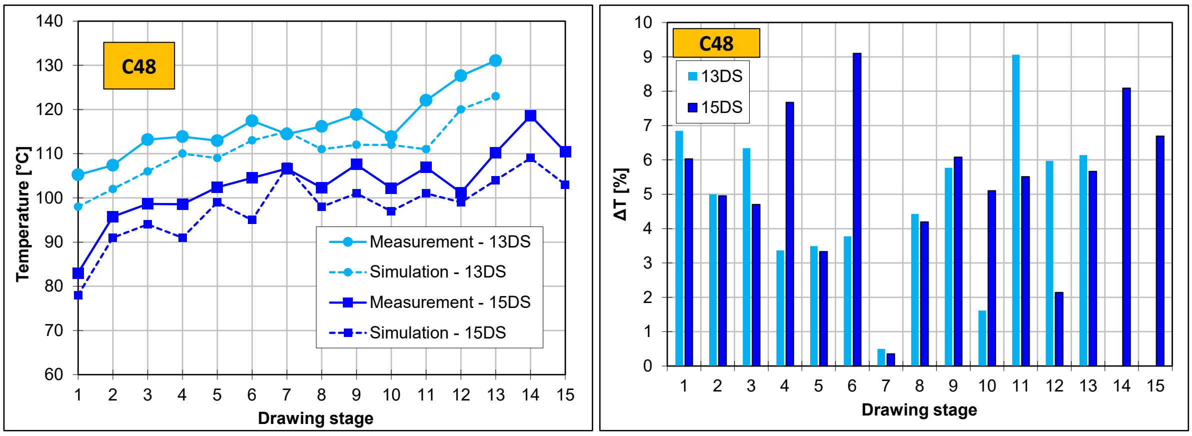

Figure 5: temperature comparison between measurement and simulation

The influence of the number of drawing stages can be seen from the temperatures shown. The lower the number of drawing steps, the higher the simulated temperatures. The deviations between measurement and simulation are less than 10%, considered over all wires of the three carbon fractions.

The comparisons between simulated and measured drawing forces and temperatures show that the simulation achieves good to very good agreements with the measured values. Individual significant differences occur only at the last two drawing stages. The cause can be assumed to be the cooling of drawing stages 15 and 16, which influences the friction conditions between wire and drawing die during the wire drawing process and leads to an increase in the drawing forces determined by measurement compared with the simulated drawing forces.

3. ANALYSIS OF MATERIAL DAMAGE DURING THE WIRE DRAWING PROCESS

Numerous drawing tests with different carbon contents and drawing sequences were carried out within the research project. The essential objective is to assess the formability of the finished wires for each drawing test as well as of the wires within the drawing tests after each drawing stage and to determine forming limits based on this. Different damage models are investigated to describe the respective residual formability. For this purpose, the calculated damage values are compared with characteristic values determined on wires with different tests and evaluated.

3.1 Principle of damage and damage models

The principle of damage is based on the assumption of the development of ductile fracture due to pore formation, pore growth and pore bonding, which ultimately leads to the failure of the material.

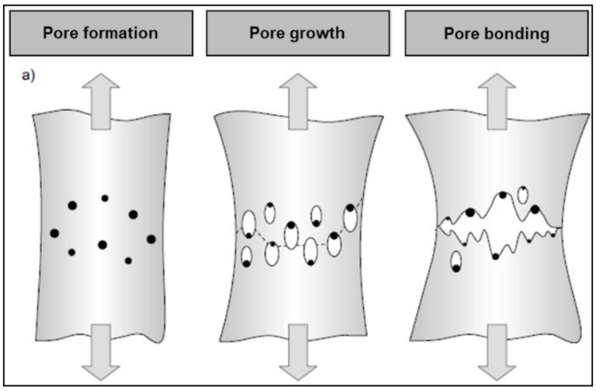

Figure 6: Principle of crack formation [1]

It is generally known from forming technology that the damage to metallic materials depends on the type of forming. If forming is performed under tension, the material is severely damaged. If forming is carried out under pressure, less damage or, depending on the material, no damage at all occurs. In addition, material damage occurs when the material is plastically deformed. Based on this principle, some damage models are known. The damage state of the material is described by stress and strain states, which are added up over the respective forming area. The damage calculations are performed in the wire center and at the wire edge for all four drawing sequences and three carbon contents. A total of seven different damage models were analyzed in the simulation [1]. While six models show a similar damage progression, the model according to Ayada is an exception. Therefore, two damage models were selected for the following investigations, the model according to Cockroft & Laytham and the model according to Ayada. The main differences between the two models lie in the choice of stress components that are used in the damage calculation. While Ayada's model takes stress triaxiality into account, Cockroft & Laytham's model evaluates the maximum principal normal stress. The equations for damage according to Cockroft and Ayada are:

$$D_{Ayada} = \int_0^{\varepsilon_V} \frac{\sigma_m}{\sigma_V}\, d\varepsilon_V \qquad (1)$$

$$D_{Cockroft} = \int_0^{\varepsilon_V} max(\sigma_1, 0)\, d\varepsilon_V \qquad (2)$$

Figure 7 shows an example of the stress plot resulting from the FE calculation for the main normal stress σ1 at drawing stage 1.

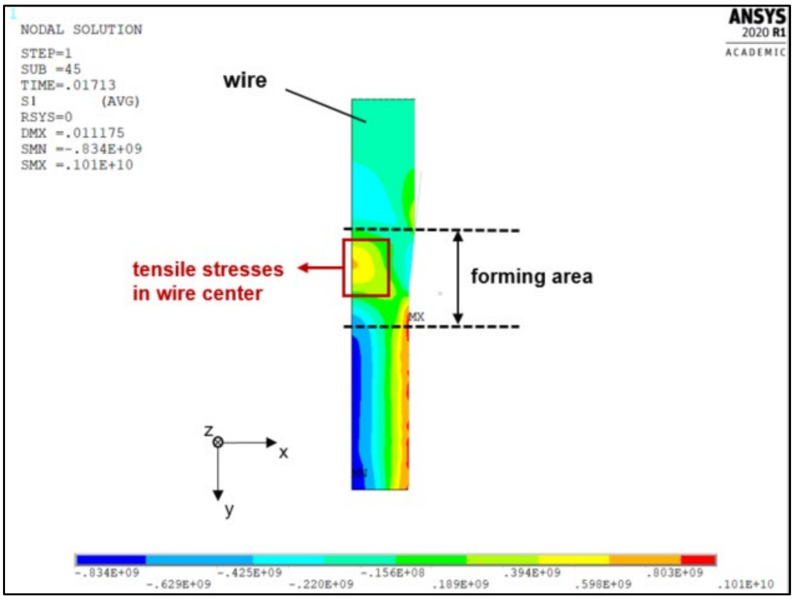

Figure 7: stress plot of the main normal stress σ1 at drawing stage 1 (FE calculation)

Damage to the wire during wire drawing occurs because of tensile stresses (in the axial direction of the wire) within the forming zone in the drawing die.
For each drawing sequence, the damage in the center of the wire and at the wire edge is calculated for each drawing stage. If the calculated damage is then plotted against the degree of deformation, the damage curves for the respective damage model are obtained. Based on the curves, both similarities and differences between the models can be determined:

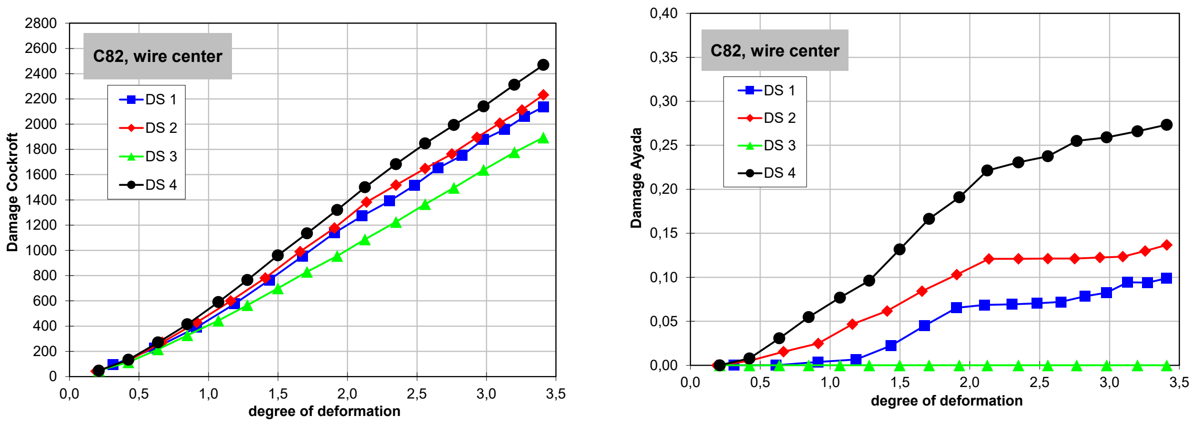

Figure 8: Damage progression versus degree of deformation; C82 wire center; **left**: Cockroft; **right**: Ayada; („DS“ = drawing sequence)

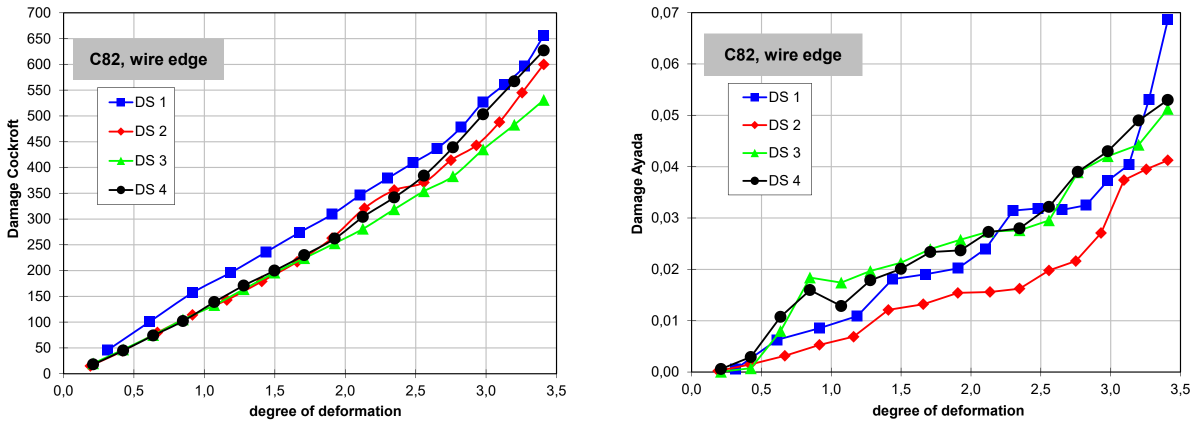

Figure 9: Damage progression versus degree of deformation; C82 wire edge; **left**: Cockroft; **right**: Ayada; („DS“ = drawing sequence)

The following key statements can be derived from the simulated damage processes:

- The damage in the center of the wire is greater than at the wire edge.
- The damage increases continuously with increasing reshaping.
- A clear dependence of the damage on the carbon content of the wires was demonstrated. The higher the carbon content, the higher the damage for the same forming.
- In particular, differences between the drawing sequences considered could be shown for the damage progressions in the wire center. This resulted in the derivation of an evaluation sequence of the drawing tests with respect to the maximum and minimum damage in the wire center, independent of carbon content and damage model.
- The model according to Ayada leaves some questions open. Damage calculated according to Ayada in the center of the wire may be zero over the entire deformation range (up to more than 95% total cross-sectional reduction). Although the model approach according to Ayada has already been used in other projects [5] [6], its suitability cannot be generally confirmed in the current research project.

3.2 Determination of critical damage values

In order to relate the simulated damage to the real wire properties, damage characteristics are derived from the practical tests (tensile test [2], torsion test [3]). The following damage characteristics are derived from the tests:

- Occurrence of multiple fractures in the torsion test
- Cracks in torsion test
- Falling below the standardized twisting number in the torsion test

Based on the test results, an attempt is made to derive a critical forming degree for each damage characteristic. For each drawing test and carbon content, those damage values are determined at which the respective damage characteristic occurs for the first time. For this purpose, the degrees of deformation at which the observed damage feature first appears (dashed lines) are plotted in the diagrams of the simulated damage processes (see Figure 8 and Figure 9).

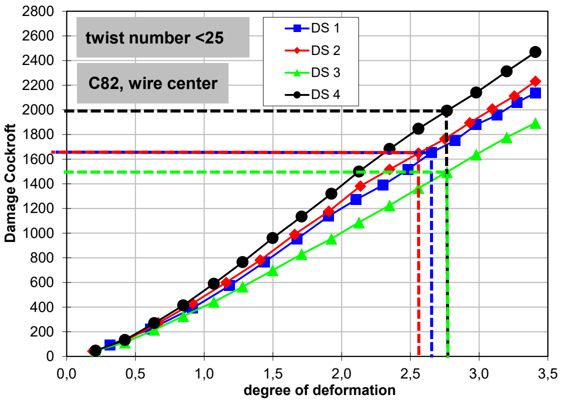

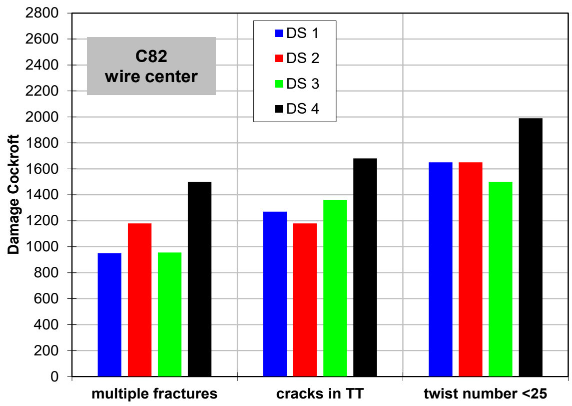

Figure 10: C82 Wire center; **left:** critical damage values when falling below the required twist number; **right:** critical damage values for other possible damage characteristics; ("DS" = drawing sequence; "TT" = tensile test)

The damage values from the left diagram are transferred to the right bar chart to facilitate the determination of critical damage values. Ideally, the bar heights per damage feature should be equal.

Deriving critical damage values by correlating the simulated damage with the damage features derived from the practical tests is only possible to a limited extent with the two damage models (Cockroft and Ayada). However, the critical damage varies differently for each damage feature of the drawing tests. In addition, the magnitude of the critical damage values depends on the carbon content. In principle, deriving critical damage values using Cockroft's simulated damage seems more reasonable than using Ayada's.

To enable a plausibility check of the investigated damage models according to Cockroft and Ayada, an FE parameter study was carried out together with corresponding validation tests on a drawing machine. Thereby, the drawing die parameters were varied at the last drawing stage (in this case drawing stage 12). This validation study is presented in the following chapter.

4. FE- PARAMETER STUDY: DETERMINATION OF DRAWING DIE GEOMETRIES FOR EXTREME VALUES OF DAMAGE AND CORRELATION WITH MECHANICAL PARAMETERS

The primary goal is to validate the two damage models used in the FE simulations (Ayada and Cockroft). A targeted variation of the drawing die geometry is carried out at a selected drawing stage, whereby the variations are derived from a statistical test plan, which is generated with the Minitab software. For each variation, FE simulations are carried out with integrated damage calculation and subsequent evaluation of the results in "Minitab". This results in drawing die geometries which lead to extreme values of the damage. After carrying out real wire drawing tests with these drawing dies, practical tests and examinations are carried out on the drawn wires. The correlation of the calculated damage with the results from the practical tests concludes of the parameter study.

4.1 Planning and execution of the parameter study

The parameter study is carried out on the 12th drawing stage with wire C82. For drawing stages 1 to 11, the drawing sequence with constant individual cross-section reduction and small drawing angle is selected (DS4-small angle), since the lowest damage in the center of the wire was calculated in the simulation. In order to reduce the number of tests or simulations to a minimum, a centrally composed test plan is used [8].

The basis of the study is the definition of influencing and target variables, as well as their range limits:

Table 1: Overview of influencing and target variables

Influencing variable or factor	Step values	Results
Half draw angle	5 levels	Drawing force Residual stresses Damage Cockroft Damage Ayada (stresses and damage each in wire center and at wire edge)
Cylinder length	5 levels	
Rounding radius	5 levels	
Single cross-section reduction (single CR)	5 levels	

Each factor is varied on 5 levels. According to the centrally composed test plan with central point, a total of 36 test points are included in the evaluation. An FE simulation is performed for each test point. The simulated values of the target variables are then transferred from "Ansys" to "Minitab".
Within Minitab, model estimation is then performed for each target variable. For each of these models, main effect and Pareto diagrams as well as extreme values can be determined. As a result, the factor combinations that lead to extreme values of the damage in each case are obtained (prognosis).
Table 2 first shows the main effect and Pareto diagrams of the selected target variables "Cockroft damage - wire center" and "Cockroft damage - wire edge". Using the main effect diagrams, the influences of the factors on the respective target variable can be determined. The Pareto diagram illustrates which factor has the greatest influence. The significance level is also shown here (vertical dashed line). Each bar that exceeds this level has a significant influence on the target variable under consideration.

Table 2: Main effect and Pareto diagrams of selected target variables.

Target	Main effect diagram	Pareto diagram
Cockroft-wire center (R^2=96%)	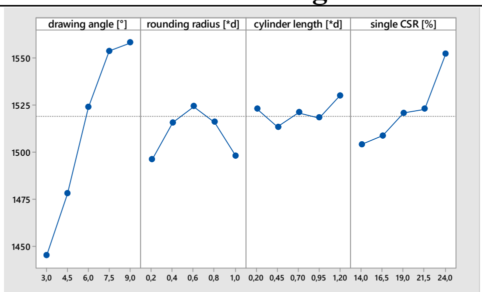	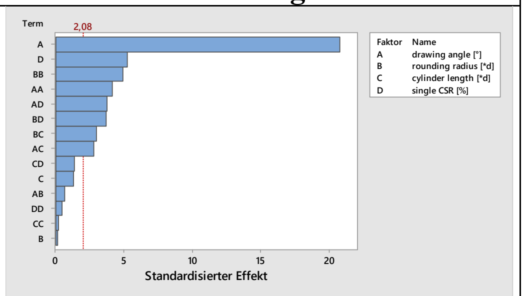
Cockroft-wire edge (R^2=95%)	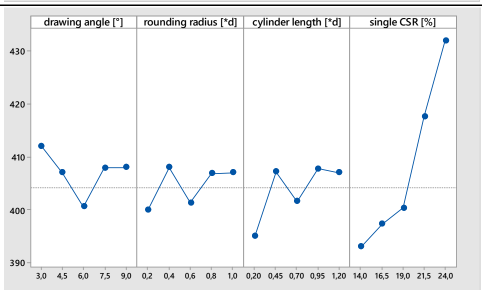	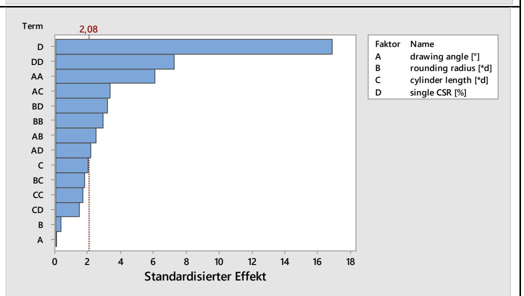

The main factor influencing Cockroft damage in the center of the wire is the drawing angle. Other influencing variables are the single cross-section reduction (single CSR for short) and the rounding radius. The greater the drawing angle, the greater the Cockroft damage in the center of the wire. The greater the single CSR, the greater the Cockroft damage in the center of the wire.

The main factor influencing Cockroft damage at the wire edge is the single CSR. Other influencing variables are the drawing angle and several interactions. The greater the single CSR, the greater the Cockroft damage at the wire edge.
In summary, it can be stated that the influencing variables drawing angle and single CSR have the most and also the largest significant effects on the target variables. Rounding radius and cylinder length influence the target values to a much lesser extent.

4.2 Correlation of simulated damage with mechanical parameters

As a further result, "Minitab" is used to determine those factor combinations, which lead to extreme values of the damage in each case (prognosis). Each factor combination corresponds to a drawing die geometry. A total of 8 drawing die geometries were specially manufactured for the validation tests. Real drawing tests were then carried out with the drawing dies on a drawing machine. The sequence of the tests followed the procedure of the FE parameter study:

- Variation of drawing die geometry at drawing stage 12 (wire C82)
- Drawing sequence for drawing stages 1 to 11: constant cross-section reduction with small angle.
- For each variation, the drawing dies at drawing stage 1 to 11 and all drawing means remain the same. The drawing die at drawing stage 12 is exchanged in each case.
- The drawing stage 12 forms the last drawing stage, after which the wire is wound directly.
- The drawing speed at drawing stage 12 is 6 m/s (corresponds to 14 m/s at drawing stage 16).

Prior to the practical tests, the derived factor combination was simulated by means of FEM. For each variation, the target variables (drawing forces, residual stresses and damage) are calculated at drawing stage 12. In particular, the simulated damages are correlated with the results from the practical tests. One test from the beginning of the test day was repeated within the study to evaluate the repeatability at the end of the test day. The reproducibility of the results was demonstrated. Figure 11 shows the simulated Cockroft damage (wire center and wire edge) for variations 1 to 8 together with the characteristic value "shear at break or crack" determined in the torsion test [3].

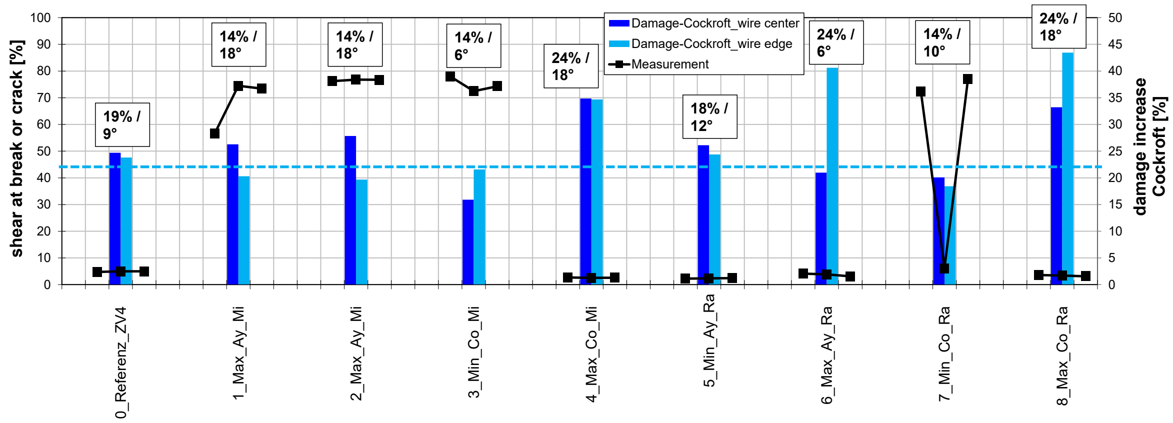

Figure 11: Correlation - damage Cockroft with characteristic value **"shear at break or crack"**

The drawn light blue dashed line represents a limit value of the edge damage. For all variations where the increase in damage at the wire edge (light blue bars) is more than 22%, the wire breaks in the torsion test. With the Cockroft model, a direct correlation between edge damage and cracking behavior in the torsion test can be derived. Such a relationship cannot be derived for the damage in the center of the wire.

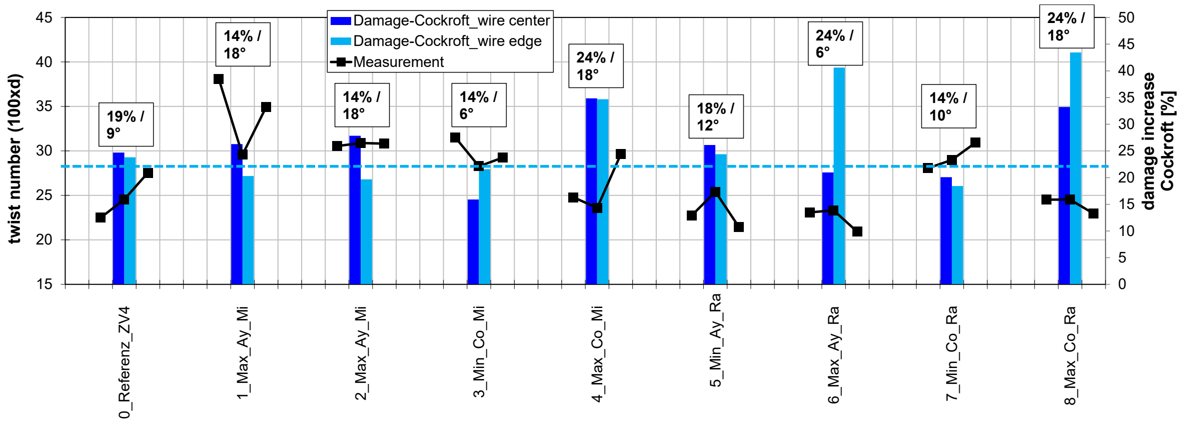

Figure 12: Correlation - damage Cockroft with characteristic value **twist number**

When looking at the twisting numbers, a similar picture emerges as in Figure 11. If the damage increases exceed the value of approx. 22% (light blue line), there is a reduction in the twist numbers compared to the variations where the edge damage increases to a lesser extent. The damage in the center of the wire again does not seem to be directly related to the twist number.
The simulated damage according to Cockroft at the wire edge allows a correlation with the mechanical parameters "displacement at break or crack" and twist number. Accordingly, a material failure in the torsion test can apparently be described by the simulated edge damage according to Cockroft.
When considering the mechanical properties from the tensile test, a correlation between total elongation at maximum force A_{gt} and the simulated damage according to Cockroft can be established. A larger increase in damage in the center of the wire is associated with a higher total elongation at maximum force A_{gt}. When looking at the wire edge, an opposite behavior can be observed.
At best, the model according to Ayada allows assumptions of a correlation. Direct correlations to the mechanical properties from the tensile and torsion tests cannot be derived with this model.

5. CONCLUSION AND OUTLOOK

The pre-curvature of the investigated wires posed a particular challenge in determining the mechanical properties, as this results in a superposition of tensile and bending stresses during the tensile test. The newly developed calculation tool for eliminating the bending stresses forms the basis for determining the $R_{p0,2}$ values and thus for the material models used in FEM and thus significantly influences the simulation results.
The comparison between measurement and simulation with regard to drawing force and temperature shows good to very good agreements.
Within the considered test space, core statements could be derived, which are independent of drawing sequence and carbon content.
The differences in damage patterns between drawing sequences within a damage model are more pronounced in the wire center than at the wire edge.
From the practical tests carried out, it was possible to determine damage characteristics and also to derive evaluation sequences with regard to formability.
By specifically varying the drawing die geometry, it was possible to determine those influencing variables, which have the greatest influence on the respective target variable.

Furthermore, a correlation between simulated edge damage and failure behavior in the torsion test was derived. This makes it possible to optimize future wire drawing processes.
Finding damage characteristics detached from standard parameters requires further investigations of the wires, especially concerning the microstructural properties. This is accompanied by the comparison of the evaluation sequences from simulation and testing with regard to damage and the determination of critical damage values.
In addition to the damage models already used in the FE simulations, the consideration of further damage models has a high research potential.

REFERENCES

[1] D. Breuer, "Bestimmung des Formänderungsvermögens bei der Kaltmassivumformung", Thesis, RWTH Aachen, 2007

[2] DIN ISO 6892-1, "Metallic materials – Tensile testing – Part 1: Method of test at room temperature", 2017

[3] DIN ISO 7800, "Metallic Materials – Wire – Simple torsion test", 2008

[4] Research topic application "Grenzen des Drahtziehens von gezogenen unlegierten Kohlenstoffstählen ohne Bleibadpatentierung", TU Ilmenau, 2018, AVIF-research project A 313

[5] R. Kaiser, "Einfluss der Ziehparameter auf die Schädigung und das Formänderungsvermögen bei der Drahtweiterverarbeitung", Thesis, Montanuniversität Leoben, 2010

[6] O. Hering, "Schädigung in der Kaltmassivumformung: Entwicklung, Auswirkungen und Kontrolle", Thesis, TU Dortmund, 2020

[7] Table presentation for the 4th project meeting „Grenzen des Drahtziehens von gezogenen unlegierten Kohlenstoffstählen ohne Bleibadpatentierung", TU Ilmenau, 2021

[8] W. Kleppmann, "Versuchsplanung", 10th revised edition, Carl Hanser Verlag, Munich, 2020

The non-profit foundation "*Stahlanwendungsforschung im Stifterverband für die Deutsche Wissenschaft e.V.*" funded the research project „Limits of wire drawing of drawn unalloyed carbon steels without lead patenting" presented. The purpose of the Foundation is to promote research in the field of steel processing and application in the Federal Republic of Germany. The research project was reviewed by a panel of experts from the „*Forschungsvereinigung der Arbeitsgemeinschaft der Eisen und Metall verarbeitenden Industrie e.V. (AVIF)*", which is made up of experts from the steel-using industry and the scientific community. A working group of the ESV ("*Eisendraht - und Stahldraht - Vereinigung e.V.*") accompanied the project.

CONTACTS

M. Sc. Christian Otto
email: christian.otto@tu-ilmenau.de
phone: (+49) 3677 69 – 3934
fax: (+49) 3677 69 – 1259